15th World Congress on Computational Mechanics (WCCM-XV)
8th Asian Pacific Congress on Computational Mechanics (APCOM-VIII)
Virtual Congress: 31 July – 5 August 2022
S. Koshizuka (Ed.)

COUPLED SIMULATION OF VIBRATIONS OF VIOLIN AND SOUND RADIATION IN CONCERT HALL

MASAO YOKOYAMA[1], AMANE TAKEI[2], RYO YOSHIDOME[2] AND GENKI YAGAWA[3]

[1] Meisei University
2-1-1 Hodokubo Hino Tokyo 191-8506 Japan
masao.yokoyama@meisei-u.c.jp, http://www.cello-maker.com/research/

[2] University of Miyazaki
1-1 Gakuen Kibanadai-nishi, Miyazaki 889-2192 Japan
takei@cc.miyazaki-u.ac.jp

[3] Toyo University and University of Tokyo
2100 Kujirai, Kawagoe, Saitama 350-8585 Japan
yagawag@gmail.com

Keywords: Violin, Time evolution, Vibration, Acoustics, Numerical simulation

Abstract. *The vibrations and the sound field around the body of an old violin made by Stradivari are studied in this paper, in which this violin is scanned using a micro-CT scanner to generate a highly precise geometric image. After the noise in the scanned data is eliminated using a computer-assisted design (CAD) software for post-processing, the geometric data are saved in the simulation software. Assuming the orthotropic properties of woods (spruce and maple), the major vibration modes of the violin, such as A0, center bout rotation, B1-, B1+, and the acoustic pressure level at the surface of the violin body are calculated using the finite element method. Next, using the sound pressure distribution at the surface of the instrument, the sound pressure spreading in a rectangular box simulating a concert hall is calculated with the open-source parallel acoustic analysis software: ADVENTURE Sound. It is concluded that the sound pressure from the violin is successfully simulated.*

1 INTRODUCTION

Owing to the high performance of computers in recent decades, numerical simulations using the finite element method (FEM) have often been conducted for the analysis of vibrations and sounds of violins [1, 2]. In addition, laser scans, as in Pezzoli et al.[3] and computed tomography (CT) scans, as in Bissinger [4], have been used to obtain three-dimensional (3D) geometric data of the violin shape.

The reason why numerical simulation has been used in the analysis of violins is that it is difficult to analyze the features of violins qualitatively and quantitatively by experiment. The differences between individual violins are significant, as violins are the products of wood-crafting. There are many variables which determine the features of the vibrations and sound due to their complex structure.

The shape and dimensions of a violin were established during the period in which Stradivari lived. However, the designs varied among violin makers, and the vibrational and acoustic features were different for each violin. Thus, numerical simulation is chosen for modelling the numerous variable factors and analyzing the vibrations and acoustic features qualitatively and quantitatively.

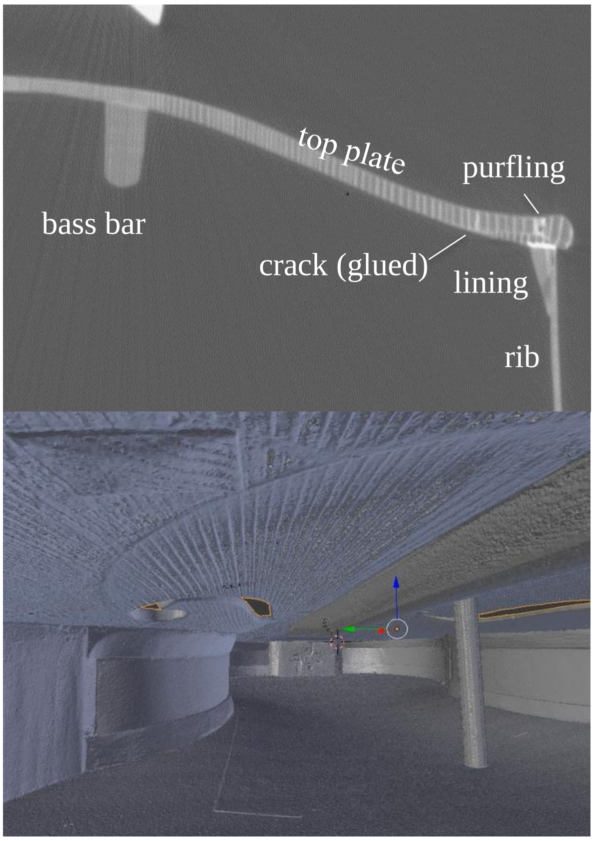

Fig. 1 Cross section from micro CT scanner image and visualization of the inside of a violin by CAD software.

Moreover, as old Italian violins are now classified as historic cultural assets, we cannot disassemble them or conduct experiments as in the past, such as the Chladni method and the impact hammering test [4, 5]. Thus, in recent years, numerical simulation has been adopted as a noninvasive technique for studying the vibrations and acoustic features of antique violins made over 300 years ago.

One of the authors conducted a coupled numerical simulation to analyze the characteristics of the vibrations and sound radiations of old violins [6]. However, the qualitative and quantitative relationships between vibrations and the acoustic field have not yet been clarified. Although coupled numerical simulations of an entire violin and its acoustic radiation have been initiated in recent years, it is too early to conclude that a sufficient outcome has been achieved.

In this study, the 3D geometry of an old Italian violin (by Antonio Stradivari in 1708) was measured using a micro-CT scanner. Then, the vibration modes of the entire violin body, including the neck, bridge, sound post, and bass bar, were calculated with the COMSOL Multiphysics code, and, using the acceleration or sound pressure on the surface of the violin body, the sound field around the violin was analyzed using the large-scale parallel software ADVENTURE Sound. Some preliminary, but interesting, results are reported herein.

2 PROCEDURES FOR NUMERICAL SIMULATION OF VIBRATIONS AND ACOUSTICS

2.1 Geometry measured by micro-CT scanner

The upper side of Figure 1 shows a cross section of the violin scanned by a micro-CT scanner, and the lower side is a snapshot visualizing the interior of the body using scanned geometric data with a computer-assisted design (CAD) software.

Here, the entire geometry of this violin by Antonio Stradivari (1708) was measured from the tail piece to the scroll of the neck with a precision of 0.1 mm. Using this scanner, we cannot only observe the parts, such as the bass bar and purfling, but also the grains of the wood and cracks, and so on in detail.

It is well known that the thicknesses of the top and back plates of a violin are generally not uniform; the central area of the plate is the thickest, and the thickness gradually decreases toward the edges.

In the numerical simulation of a violin, the detailed geometric data of the real thickness measured by a micro-CT scanner is important, and meaningful calculation results cannot be obtained if this gradation in the real thickness is not considered [3, 6].

Because the data from the CT scanner includes many fragments and noise, we have to remove all of these using CAD software for post-processing. The geometric data are divided into parts such as top/back plate, rib, sound post in order to determine each physical property and saved in the standard for the exchange of product model data (STEP) format.

2.2 Vibration analysis of violin body by FEM

The meshing and vibration analyses of the violin body were performed using the COMSOL Multiphysics code. The STEP files of the violin described in Section 2.1 were imported to COMSOL Multiphysics as a geometric object. In COMSOL Multiphysics, the mesh generators discretize the domains into tetrahedral second-order mesh elements using the free-mesh method [7]. The total number of elements is approximately 2 million, including both violin and air, and the eigenmode, displacement, and sound pressure on the surface of the violin are calculated via the acoustic-structure interaction module of COMSOL Multiphysics using FEM. Free vibrations were calculated without any constraint points at the surface of the violin.

In COMSOL Multiphysics, the physical characteristics of wood can be set in the three orthogonal directions: the longitudinal grain direction (x-axis), the radial annual ring direction (y-axis), and the direction tangential to the annual ring (z-axis). The violin plate was sawed, as shown in Fig. 3.

As listed in Table I, the typical values measured by Green et al.[8] are referred to for the orthotropic properties (Young’s modulus, rigidity modulus, and Poisson’s ratio). Here, Ey/Ex, Ez/Ex, and the rigidity modulus (G/Ex) indicate the ratios of the longitudinal Young’s modulus Ex. The value of EL is also cited from [8]; the Ex value of maple is 12.6 GPa, and that of spruce is 9.9 GPa. The density is 0.63 for maple and 0.36 for spruce. However, these values are different from the actual values of the scanned violin . In future work, we intend to develop a method for measuring the material properties of old violins for numerical simulation.

Table 1 Values of orthotropic properties employed in the numerical simulation [8]. Ex value of maple is 12.6 GPa, and that of spruce is 9.9 GPa.

Property	Maple	Spruce
Young's modulus E_Y / E_X	0.132	0.078
E_Z / E_X	0.065	0.043
Rigidity modulus G_{XY} / E_X	0.111	0.064
G_{YZ} / E_X	0.021	0.003
G_{XZ} / E_X	0.063	0.061
Poisson's ratio μ_{XY}	0.424	0.372
μ_{YZ}	0.774	0.435
μ_{XZ}	0.476	0.467

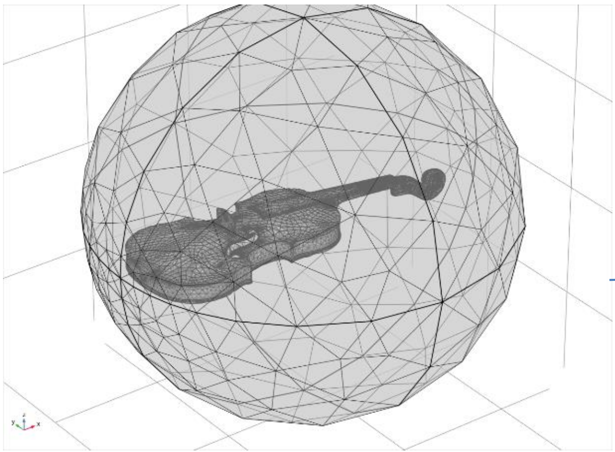

Fig. 2 Mesh of violin and air field by auto-mesh function of COMSOL Multiphysics.

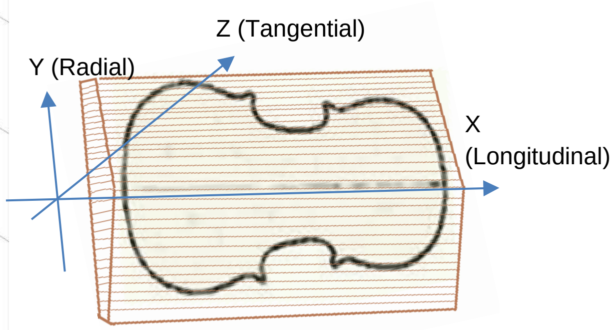

Fig. 3 Setting of orthotropic directions in violin plate.

2.3 Large scale computing of sound radiation

The pressure and coordinate data on the surface of the violin in COMSOL were passed to ADVENTURE_Sound[9]. In ADVENTURE_Sound, the iterative domain decomposition method (IDDM) was applied. IDDM is the most efficient parallel technique for large-scale analysis, with several hundred million to several billion degrees of freedom, implemented by the hierarchical domain decomposition method (HDDM)[10]. In HDDM, the original analysis domain is first divided into parts, which are further decomposed into smaller domains called subdomains. Parts and subdomains are assigned to each calculation node. Then, the iterative calculation of the COCG method for the interface problem begins. In each step of the COCG method, the subdomain problem is solved using the Gaussian elimination method by changing the boundary condition for the interface problem. The HDDM algorithm is shown in Fig. 4. The convergence criteria for the interface and subdomain problems were set to ε=1.0e-07 and δ =1.0e-09, respectively. These criteria were defined to obtain a balance between the accuracy of the solution and the calculation time.

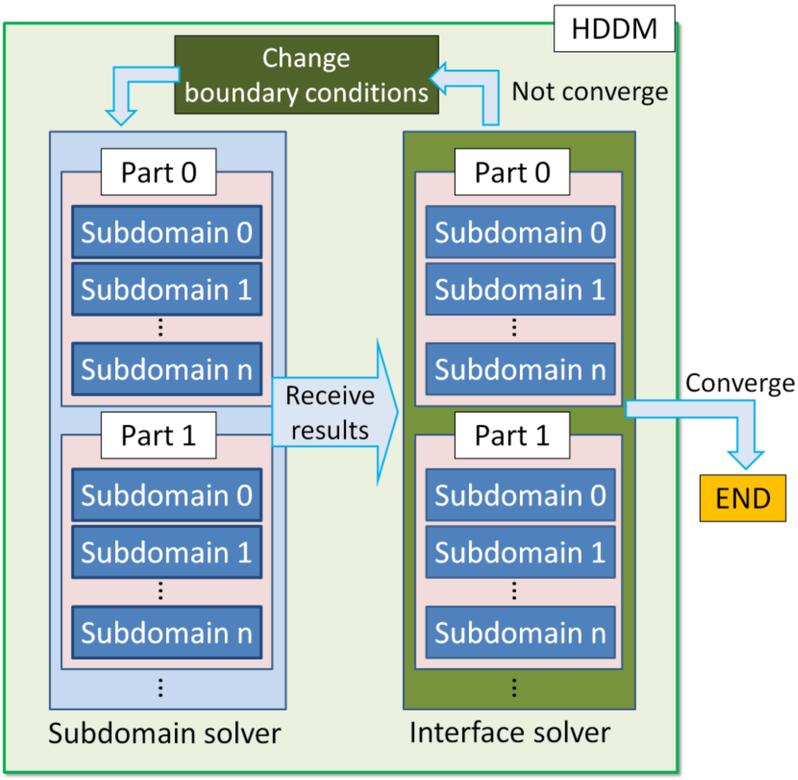

Fig. 4 Algorithm of HDDM

3 SIMULATION RESULTS

3.1 Vibration modes of violin

Regarding the vibration analysis of the violin body, eigenmodes at low frequencies under 1000 Hz are often discussed to analyze the characteristics of violins[11,12]. Mode A0 is a basic vibration mode called the air cavity mode near 280 Hz, whereas B1- and B1+ are the corpus bending modes appearing at both the top and back plates. These modes are significantly related to sound radiation and volume. Another mode is the center bout rhomboid/rotation (CBR), which is a twist mode in the center bouts of the violin body without significant influence on the sound radiation [11].

The displacements in the z-axis direction node lines of the (a) A0, (b) CBR, (c) B1-, and (d) B1+ modes are shown in Fig. 5. The red area indicates where the displacement is positive and the blue area indicates where the displacement is negative. The eigenfrequencies of each mode are 275.4 Hz (A0), 425.8 Hz (CBR), 427.1 Hz (B1 −), and 494.7 Hz (B1+). Though the frequencies of B1-/B1+ modes are lower than other literatures, these differences are caused by the setting of the parameters in the calculation.

Figure 6 depicts the sound pressure field around the body in the A0 mode. The left-hand side of the figure shows the displacement fields in the x-y plane 50 mm above the top plate, and the right-hand side of the figure shows the y–z plane at the sound post from the viewpoint of the neck of the violin.

From the simulation results, it can be confirmed that when the top plate expands and contracts in the A0 mode, the area at the bass bar fluctuates significantly, and the wing of the f-hole vibrates significantly. Furthermore, the high acoustic pressure around the f-hole indicates the influence of the f-holes on sound radiation. These results are in good agreement with the experimental observations.

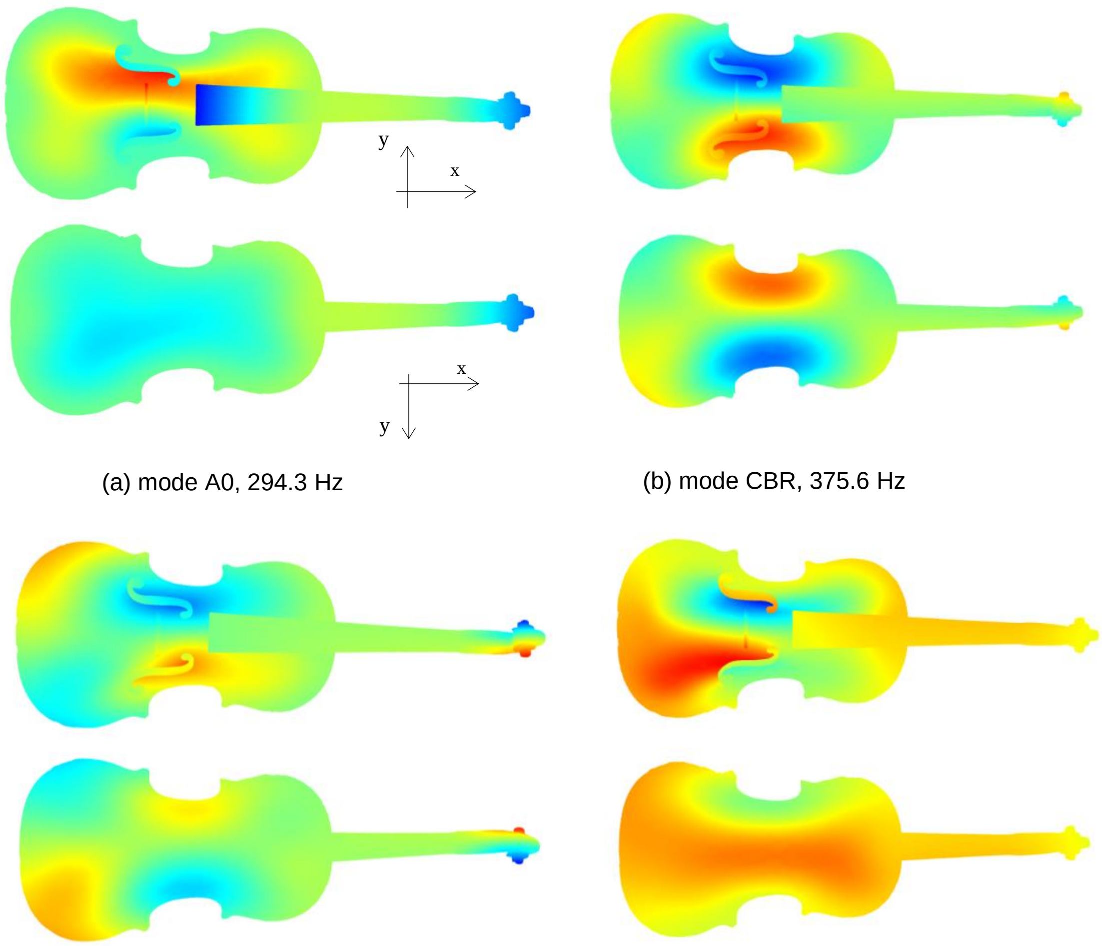

(a) mode A0, 294.3 Hz

(b) mode CBR, 375.6 Hz

(c) mode B1-, 427.1 Hz

(d) mode B1+, 494.7 Hz

Fig. 5 Displacements in modes A0, CBR, B1-, and B1+. The red area represents the positive value in the z direction and the blue area represents the negative z direction.

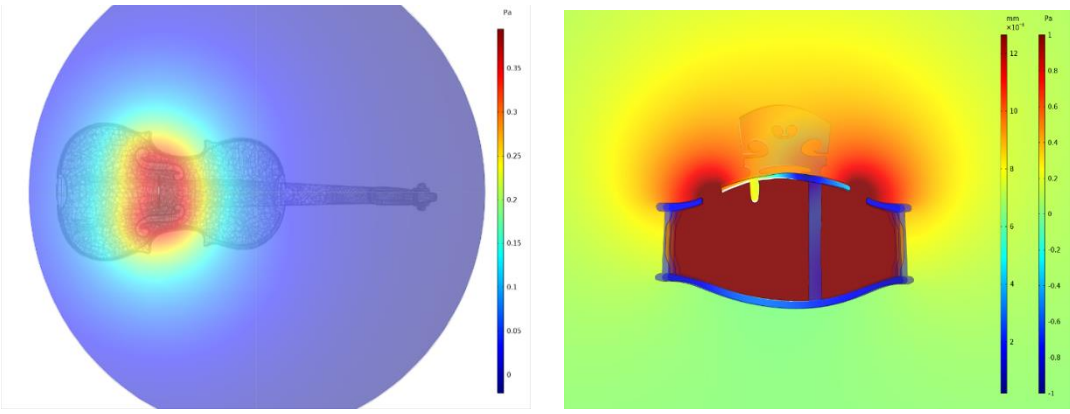

Fig. 6 Acoustic pressure fields around the violin body in mode A0. The blue area in the contour map represents a low-pressure level, and the red area represents a high-pressure level.

Table 2 Numerical analysis by ADVENTURE_Sound

Frequency [kHz]	0.5	1.0	1.5	2.0
Iterative count	1199	1502	3427	4384
Elapsed time [s]	2154	2714	3781	4880

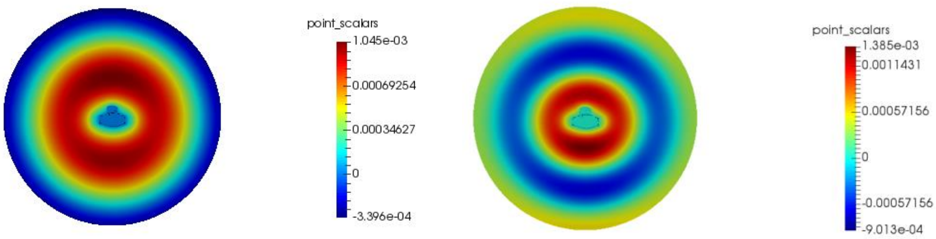

(a) 0.5 kHz (b) 1.5 kHz

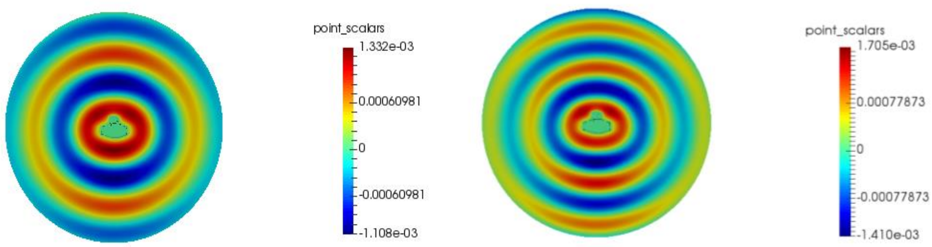

(c) 1.5 kHz (d) 2.0 kHz

Fig. 7 Visualization of sound radiation by ADVENTURE_Sound.

3.2 Sound radiation in a wide space

The violin was then wrapped by a spherical air domain, and the results of the analysis using the parallel acoustic analysis code (ADVENTURE_Sound) for frequencies 0.5, 1.0, 1.5, and 2.0 kHz are shown in Table 2 and visualized in Figs. 7(a), (b), (c), and (d). As a boundary condition, sound absorption was set to the surface of the sphere. A PC cluster (Intel Core i7-2600 3.40 GHz, 32 GB Mem/Node, 25 node) was used for the calculations. These results demonstrate that it is possible to calculate the radiation phenomenon of sounds from a violin surface to the air domain around the violin.

4 CONCLUSION

The coupled simulation of the mode vibrations and the sound radiation of a violin scanned by a micro-CT scanner was conducted using FEM. A preliminary simulation of the sound radiation in a concert hall was performed using the parallel acoustic analysis code (ADVENTURE_Sound). Currently, the implementation of a program for a large-scale analysis using the acoustic pressure on the surface of a violin body is under development. The dynamic analysis of sound radiation from forced vibrations on the bridge of a violin in a hall will be calculated in the near future.

ACKNOWLEDGMENTS

I would like to thank Bunkyo-Gakki Co., Ltd. for providing violins, and Editage (www.editage.com), for English language editing. This work was supported by JSPS KAKENHI Grant Number 21K11969.

REFERENCES

[1] Gough, C. (2021). Acoustic characterization of string instruments by internal cavity measurements. The Journal of the Acoustical Society of America, 150(3), 1922-1933.

[2] Torres, J. A., Soto, C. A., & Torres-Torres, D. (2020). Exploring design variations of the titian Stradivari violin using a finite element model. The Journal of the Acoustical Society of America, 148(3), 1496-1506.

[3] Pezzoli, M., De Lucia, R. R., Antonacci, F., and Sarti, A. "Predictive simulation of mechanical behavior from 3D laser scans of violin plates." Proceedings of International Conference on Acoustics 2019 (2019).

[4] Bissinger, G. and Oliver, D. "3-D laser vibrometry on legendary old Italian violins." Sound and Vibration 41.7 (2007): 10-15.

[5] Hutchins, C.M. and Benade V., “Research papers in violin acoustics, 1975-1993: with an introductory essay, 350 years of violin research” Vol. 1. The Acoustical Society of America (1997).

[6] Yokoyama, M. "Coupled numerical simulations of the structure and acoustics of a violin body." The Journal of the Acoustical Society of America 150.3 (2021): 2058-2064.

[7] Acoustic-Structure Interaction, COMSOL Homepate, https://www.comsol.jp/model/acoustic-structure-interaction-417.

[8] Green, D. W., Winandy, J. E., and Kretschmann, D. E. "Mechanical properties of wood. Wood handbook: wood as an engineering material" Madison, WI: USDA Forest Service, Forest Products Laboratory, 1999. General technical report FPL; GTR-113: (1999): 4.1-4.45, 113.

[9] ADVENTURE Project home page: https://adventure.sys.t.u-tokyo.ac.jp/ (Access on 15 Nov. 2021) .

[10] Kudo A. and Takei A,, "Performance evaluation of wave-sound analysis code: ADVENTURE Sound," Proceedings of The 40th JSST Annual Conference: International Conference on Simulation Technology, Kyoto, Japan, Sep. 1-3, 2021.

[11] Woodhouse J., "The acoustics of the violin: a review," Reports on Progress in Physics 77.11 (2014): 115901.

[12] Pyrkosz, M., & Van Karsen, C. (2013). Comparative modal tests of a violin. Experimental Techniques, 37(4), 47-62.